Low-complexity Optimized Version of AOR Algorithm for Signal Precoding in Large-scale MIMO Systems

Naceur Aounallah and Smail Labed

Kasdi Merbah Ouargla University, Ouargla, Algeria

https://doi.org/10.26636/jtit.2025.4.2281

Abstract — In recent years, there has been a growing focus on research concerning wireless communication technologies, with a particular emphasis placed on the emerging field of massive MIMO systems. In these systems, precoding performed at the base station (BS) is a crucial signal processing task which ensures reliable downlink transmission. In this paper, we propose a new modified accelerated overrelaxation (AOR) approach to enhance signal precoding in large-scale MIMO downlink systems. This approach uses distinctive matrix decompositions along with optimally selected relaxation and acceleration parameters. Specifically, the proposed method, termed "optimized symmetric accelerated over-relaxation (OSAOR)", exhibits two key advantages: low complexity (compared to the near optimal zero forcing (ZF) precoder) and iterative nature, with its parameters optimized by means of the particle swarm optimization (PSO) algorithm that is capable of boosting convergence and improving precoding precision. Simulation results are given to confirm the superiority of the proposed algorithm, as it may outperform conventional AOR and other existing solutions.

Keywords — AOR iteration, linear precoders, low complexity, massive MIMO, PSO algorithm

1. Introduction

In recent years, research focusing on the field of communications has revealed that the full potential of MIMO systems to achieve high spectral efficiency remains underutilized in practical applications. As a result, the large-scale MIMO (LS-MIMO) approach, commonly referred to as massive MIMO, has emerged as a promising solution to address this limitation. This technology involves equipping base stations with large antenna arrays that contain tens to hundreds of elements, thus enabling simultaneous communication with multiple terminals over the same time-frequency resources.

Using this approach, massive MIMO significantly enhances spectral efficiency, allowing higher data rates without increasing bandwidth. Furthermore, it provides substantial benefits in terms of capacity, energy efficiency, and link reliability, making it a key enabler for 5G and beyond wireless networks [1]. As demand for high-speed, low-latency and ultra-reliable communication continues to grow, massive MIMO stands out as a transformative wireless access technology poised to meet the evolving needs of next-generation communication systems [2], [3].

In addition to the promising advantages, several practical challenging problems must be solved to realize a massive MIMO system, with precoding performed in the system's downlink portion being one of them. Consequently, a plethora of massive MIMO precoding methods has been proposed to reach a satisfactory trade-off between overall performance and the complexity of the solution.

In fact, precoding methods can be categorized as linear or non-linear, depending on whether they involve non-linear operations in their computation. Non-linear precoding techniques, such as constant envelope (CE), dirty paper coding (DPC) [4], vector perturbation (VP), lattice-aided methods, and Tomlinson-Harashima precoding (THP) are generally impractical for hardware implementation due to their high computational complexity [5]. As a result, linear precoding techniques, including matched filter (MF), zero-forcing (ZF), and minimum mean square error (MMSE) are preferred and considered as benchmark linear precoders. However, these methods require that the channel matrix, including all user data, be inversed [6].

To address high computational complexity associated with large-scale matrix inversion, several alternative linear precoding methods have been proposed. These methods generally fall into three main categories: direct methods, iterative methods, and expansion methods. Direct methods transform the matrix requiring inversion into a product of simpler matrices, such as QR or Cholesky decomposition [7]. Although accurate, these methods suffer from high computational complexity.

Iterative methods solve linear equations through successive approximations and include techniques such as the Richardson method [8], the conjugate gradient (CG) method [9], and successive over-relaxation (SOR) [10]. These approaches are computationally efficient for large-scale systems, but may require careful parameter tuning for fast convergence.

Expansion methods approximate the matrix inverse using a series of matrix vector products, with examples including the Neumann series (NS) [11], the truncated polynomial expansion (TPE), as well as Newton iteration (NI) and Chebyshev iteration (CI) algorithms [12], [13]. These approaches provide a trade-off between complexity and accuracy, making them particularly suitable for massive MIMO systems.

Conventional quasi-optimum precoders, such as zero forcing (ZF) and minimum mean square error (MMSE) [14], achieve the best BER performance. However, they require matrix inversion calculation, which leads to high computational complexity.

To address this challenge, researchers have explored iterative algorithms to overcome the need for direct matrix inversion in mathematical operations [15]. The accelerated overrelaxation (AOR) method, introduced in [16], is one of such approaches. It bypasses the operation of the inverse matrix through linear iteration, thus reducing computational complexity from $\mathcal{O}(U^3)$ to $\mathcal{O}(U^2)$. Despite this improvement, AOR performance remains suboptimal and requires further enhancement. In response, the authors of [17] proposed the symmetric accelerated over-relaxation (SAOR) method, which builds upon AOR by incorporating two similar symmetric matrices for iteration, leading to improved performance over the original AOR method.

Building on these developments, recent research has focused on further improvement of iterative AOR-based precoding schemes. For example, in [18], an improved AOR-based precoding method was introduced, where the acceleration factor of AOR is optimized using the relationship between the spectral radius and the eigenvalues of a positive definite Hermitian matrix, which depends solely on the number of transmitting and receiving antennas.

In addition, article [19] presents an improved variant of the traditional AOR method, termed optimized AOR (OAOR). This approach integrates a novel variant of meta-heuristic particle swarm optimization (PSO), refining the cognitive coefficients to optimize the relaxation parameters for OAOR. Furthermore, the AOR iterative method, which is applicable both to massive MIMO detection and precoding, has been further refined in [20] using the Nelder-Mead simplex optimization technique. This heuristic optimization approach facilitates the determination of optimal acceleration and relaxation parameters, leading to higher detection accuracy and faster convergence.

The main contribution of this work is the proposition of a new version of the accelerated over-relaxation (AOR) algorithm that is used as a linear precoder for massive MIMO systems. The new solution is referred to as the optimized symmetric accelerated over-relaxation (OSAOR) algorithm. The proposed scheme is developed by integrating the strengths of the symmetric accelerated overrelaxation (SAOR) method and the PSO algorithm.

The primary objective of employing PSO is to find the optimal values of relaxation and acceleration parameters for the SAOR precoder. We analyze the computational complexities of SAOR and OSAOR precoders and compare them with those of the near-optimal ZF precoder. Additionally, we discuss the influence of the relaxation and acceleration parameters on the convergence speed of the proposed OSAOR method.

The remainder of the paper is organized as follows. In Section 2, we describe the multi-user large MIMO downlink system model, formulate the precoding problem, and review the ZF benchmark precoder. Then, in Section 3, the classical AOR detection algorithm is reviewed and its new version is proposed. Computational complexity is studied in Section 4, and the numerical results allowing to compare the performance of the proposed approach are analyzed in Section 5. The latter is followed by conclusions and future perspectives presented in Section 6.

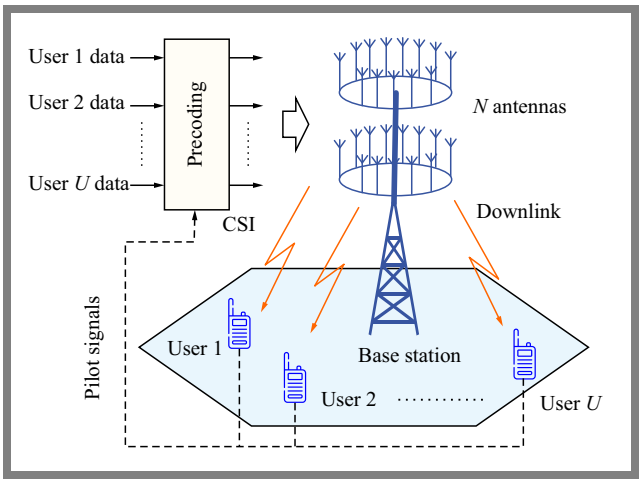

Fig. 1. Model of a massive MIMO downlink system with U single antenna users and N BS antennas.

2. System Description and Problem Formulation

This section examines the downlink transmission of a large-scale multi-user MIMO system, where each base station (BS) is fitted with N antennas and serves concurrently U single-antenna users within the same frequency band, with $U \ll N$ [1]. We assume that the base station has perfect knowledge of channel state information (CSI), which can be obtained through pilot-based training [21]. For this communication scenario, we consider the Rayleigh flat-fading channel model. A model of the system is shown in Fig. 1.

The received signal vector $y \in C^{U\times 1}$ at the user terminals can be mathematically described as follows:

$$y = \sqrt{\rho_r}\, H\, x + n\,, \tag{1}$$

where $\sqrt{\rho_r}$ is a normalization factor to determine signal to noise power ratio (SNR), $H \in C^{U\times N}$ is the channel matrix, $x \in C^{N\times 1}$ is the transmitted symbol vector, and $n \in C^{U\times 1}$ is the complex additive white Gaussian noise (AWGN) vector at the receiver with zero mean and σ^2 variance.

The considered system model can be represented in a matrix form as:

$$\begin{bmatrix} y_1 \\ y_2 \\ y_3 \\ \vdots \\ y_U \end{bmatrix} = \sqrt{\rho_r} \begin{bmatrix} h_{11} & h_{12} & \dots & h_{1N} \\ h_{21} & h_{22} & \dots & h_{2N} \\ h_{31} & h_{32} & \dots & h_{3N} \\ \vdots & \vdots & \ddots & \vdots \\ h_{U1} & h_{U2} & \dots & h_{UN} \end{bmatrix}^T \begin{bmatrix} x_1 \\ x_2 \\ x_3 \\ \vdots \\ x_N \end{bmatrix} + \begin{bmatrix} n_1 \\ n_2 \\ n_3 \\ \vdots \\ n_U \end{bmatrix} . \tag{2}$$

Each entry h_{ij} of channel matrix H is modeled as an independent and identically distributed (i.i.d.) complex Gaussian random variable according to $\mathcal{CN}(0,1)$ distribution, while the AWGN vector entries are i.i.d., with each of them following $\mathcal{CN}(0,\sigma^2)$ distribution.

In practice and under nonideal conditions, the assumption of perfect CSI at the BS is rarely achievable due to noisy channel estimation and pilot contamination. To model this, the estimated channel matrix $\hat{H}$ can be represented as [22]:

$$\hat{H} = \sqrt{1-\tau^2}\, H + \tau H_e \,, \tag{3}$$

where H denotes the true channel matrix with i.i.d. entries following $\mathcal{CN}(0,1)$, $H_e \in C^{U\times N}$ being the estimation error matrix with i.i.d. entries also distributed as $\mathcal{CN}(0,1)$, and $0 \leqslant \tau \leqslant 1$ controlling the quality of CSI.

The challenge of signal precoding in massive MIMO at the base station is to optimize the transmitted signal vector x, so that users receive their intended signal via the received vector y with minimal interference.

Therefore, the base station applies a precoding matrix $W \in C^{N\times U}$ to the original data symbols $s \in C^{U\times 1}$ intended for users, leading to:

$$x = Ws \,. \tag{4}$$

Thus, the received signal becomes:

$$y = \sqrt{\rho_r}\, HWs + n = \sqrt{\rho_r}\, Q\, s + n \,, \tag{5}$$

where $Q = HW$ represents the equivalent channel matrix, and making it close to an identity matrix helps minimize multi-user interference.

The signal-to-interference plus noise ratio (SINR) at the u-th reception can be given to the user as follows [23]:

$$SINR_u = \frac{\frac{\rho_r}{U}\,|q_{u,u}|^2}{\frac{\rho_r}{U}\sum\limits_{m\neq n}^{U}|q_{m,u}|^2 + 1} = \frac{\rho_r}{U}\,|q_{u,u}|^2 \,, \tag{6}$$

where $q_{m,u}$ denotes the element of matrix Q at the intersection of the m-th row and the u-th column.

The ergodic capacity of the downlink massive MIMO system after applying precoding can be expressed as [22]:

$$C = \sum_{u=1}^{U} \log_2(SINR_u + 1) \,. \tag{7}$$

The achievable capacity is a key factor in assessing the performance of precoding techniques.

In this study, the basic zero forcing (ZF) precoding algorithm is used as a benchmark linear precoder. Its primary objective is to mitigate interuser interference by adhering to optimization criteria designed to minimize it [24]. The corresponding ZF precoding matrix is the following:

$$W_{ZF} = \beta\, H^H (HH^H)^{-1} = \beta\, H^H G^{-1} \,, \tag{8}$$

where $G = HH^H$ stands for the Gram matrix, while β is the normalization parameter that accounts for the average fluctuations in transmit power. This parameter is defined as:

$$\beta = \sqrt{\frac{U}{tr(G^{-1})}} \,, \tag{9}$$

The transmitted signal, after ZF precoding has been applied, can be represented as:

$$x_{ZF} = W_{ZF} s = \beta\, H^H G^{-1} s = \beta\, H^H z \,, \tag{10}$$

where $G^{-1}s = z$, which clearly results in:

$$G\, z = s \,. \tag{11}$$

The vector of the received signals after applying ZF precoding is given by:

$$y_{ZF} = \beta\sqrt{\rho_r} HH^H (HH^H)^{-1} s + n = \beta\sqrt{\rho_r} Es + n \,, \tag{12}$$

where $E = HH^H(HH^H)^{-1}$ is the ZF equivalent channel matrix. Then, the corresponding signal-to-interference-plus-noise ratio (SINR) for any u-th user can be determined as [22], [23]:

$$\begin{aligned} SINR_u &= \frac{\frac{\rho_r}{U}|e_{u,u}|^2}{\frac{\rho_r}{U}\sum\limits_{m\neq u}^{U}|e_{m,u}|^2 + 1} \\ &= \frac{\rho_r}{U}\left|e_{u,u}\right|^2 = \frac{\rho_r}{tr(G^{-1})} \,, \end{aligned} \tag{13}$$

where $e_{m,k}$ represents the element of matrix E located in the m-th row and the k-th column.

Based on Eq. (13), the sum capacity achieved by ZF precoding in a large-scale MIMO system can be determined using the following expression [23], [25]:

$$\begin{aligned} C_{ZF} &= \sum_{u=1}^{U} \log_2(SINR_u + 1) \\ &= U \log_2\left(\frac{\rho_r}{tr(G^{-1})} + 1\right) \,. \end{aligned} \tag{14}$$

3. Precoding Algorithms

3.1. Standard AOR

The standard accelerated over-relaxation (AOR) splitting method was originally proposed in [16] as a two parameter linear stationary method for solving linear systems of the $x = A^{-1}\, b$ form. Hadjidimos demonstrated that when these two parameters are appropriately chosen, the AOR method achieves faster convergence compared to other similar approaches.

The AOR method has been proven to be a powerful tool for solving problems associated with linear systems [18]. To explicitly formulate the iterative process of the AOR method, we start by decomposing the precoding matrix W from Eq. (4) into its fundamental components as follows:

$$W = W_D - W_L - W_U \,, \tag{15}$$

where W_D represents the diagonal part of W, while $-W_L$ and $-W_U$ correspond to the strictly lower and strictly upper triangular parts, respectively.

Using this decomposition, we can now reformulate the original Eq. (4) as follows:

$$(W_D - W_L - W_U)\, x = s \,. \tag{16}$$

Rewrite this equation:

$$W_D\, x = W_L\, x + W_U\, x + s\,. \tag{17}$$

We apply W_D^{-1}, the inverse of the diagonal matrix W_D, to both sides and simplify the left side, since $W_D^{-1}\, W_D = I$:

$$x = W_D^{-1}(W_L\, x + W_U\, x + s)\,. \tag{18}$$

At this stage, we incorporate the relaxation parameter $\omega \in R$:

$$x = x + \omega\left(W_D^{-1}(W_L\, x + W_U\, x + s) - x\right). \tag{19}$$

Expanding the equation, the following form is obtained:

$$x = x + \omega\,(W_D^{-1}\, W_L\, x + W_D^{-1} W_U\, x + W_D^{-1} s - x)\,. \tag{20}$$

Next, we introduce the acceleration parameter $\gamma \in R$:

$$x = x + \omega\,(\gamma\, W_D^{-1} W_L\, x + W_D^{-1} W_U\, x + W_D^{-1} s - x)\,. \tag{21}$$

Reorganizing the terms:

$$x = (1-\omega)\, x + \omega\,\gamma\, W_D^{-1} W_L\, x + \omega\, W_D^{-1} W_U\, x + \omega\, W_D^{-1} s\,. \tag{22}$$

We extract x as a common factor:

$$x = \left[(1-\omega) I + \omega\,\gamma\, W_D^{-1} W_L + \omega\, W_D^{-1} W_U\right] x + \omega\, W_D^{-1} s\,. \tag{23}$$

To formulate this as an iterative method, we introduce the iteration index i:

$$x^{(i+1)} = \left[(1-\omega) I + \omega\,\gamma\, W_D^{-1} W_L + \omega\, W_D^{-1} W_U\right] x^{(i)} + \omega\, W_D^{-1} s\,. \tag{24}$$

To simplify the computation, we multiply both sides by $(W_D - \gamma W_L)$:

$$\begin{aligned}(W_D - \gamma W_L)\, x^{(i+1)} = \big[&(1-\omega) W_D + (\gamma - \omega) W_L \\ &+ \omega\, W_U\big] x^{(i)} + \omega\, s\,.\end{aligned} \tag{25}$$

Finally, solving for $x^{(i+1)}$, we derive the AOR iteration formula:

$$\begin{aligned}x^{(i+1)} = (W_D - \gamma\, W_L)^{-1}\big(\big[&(1-\omega) W_D \\ &+ (\gamma - \omega) W_L + \omega\, W_U\big] x^{(i)} + \omega\, s\big)\,.\end{aligned} \tag{26}$$

The optimal relaxation parameter ω and the optimal acceleration parameter γ of the AOR iterative method are given by [26] as follows:

$$\omega = \frac{2}{1 + \sqrt{1 - \mu_{max}^2}}\,, \tag{27}$$

$$\gamma = \frac{\mu_{max}^2 - \mu_{min}^4}{\mu_{max}^2 (1 - \mu_{min}^2)}\,, \tag{28}$$

where μ_{max} and μ_{min} denote the maximum and the minimum eigenvalues of the Jacobi matrix, respectively.

3.2. Symmetric AOR Version

The symmetric accelerated over-relaxation (SAOR) method can be interpreted as a double sweep approach. The first sweep follows the standard AOR method, while the second sweep applies the AOR method with the roles of W_L and W_U matrices interchanged.

In other words, each iteration of the SAOR method consists of two half-iterations: a forward pass using the AOR method, followed by a backward pass where the equations are processed in a reverse order, effectively applying AOR again.

Therefore, the SAOR iterative process is executed in the two steps described below:

1) Perform the first half iteration, which is equivalent to the AOR iteration [16], as follows:

$$\begin{aligned}x^{(i+1/2)} = (W_D - \gamma W_L)^{-1}\big(\big[&(1-\omega) W_D \\ &+ (\gamma - \omega) W_L + \omega\, W_U\big] x^{(i)} + \omega\, s\big)\end{aligned}\,. \tag{29}$$

2) Perform the second half iteration, applying the AOR method with the equations processed in a reverse order, as follows:

$$\begin{aligned}x^{(i+1)} = (W_D - \gamma\, W_U)^{-1}\big(\big[&(1-\omega) W_D \\ &+ (\gamma - \omega)\, W_U + \omega\, W_L\big]\, x^{(i+1/2)} + \omega\, s\big)\,.\end{aligned} \tag{30}$$

In SAOR-based precoding, both relaxation ω and acceleration γ parameters are within the range of $[0, 2]$, serving the same role as in AOR. Their optimal values can be determined using Eqs. (27) and (28).

3.3. Improved Version of SOAR

The performance of the SAOR version is strongly influenced by its acceleration and relaxation parameters. To systematically determine these parameters, we integrate an innovative approach based on the PSO algorithm. This heuristic method enables the identification of optimal values, ensuring enhanced precoding accuracy and faster convergence, even in complex system configurations.

So, to determine the optimal ω and γ for improving the performance of the SAOR method, we formulate an optimization problem as follows:

$$\begin{aligned}&\text{minimize} \quad f(\omega, \gamma) = \mathbb{E}\left[||x - \hat{x}(\omega, \gamma)||^2\right] \\ &\text{subject to} \quad 0 < \omega < 2, \quad 0 < \gamma < 2 \\ &\rho\left(I - \omega\, W_D^{-1} G^H G + \omega\,\gamma\, {W_D}^{-1}(W_D - W_L - W_U)\right) < 1\end{aligned} \tag{31}$$

where $\rho(\cdot)$ denotes the spectral radius of a matrix.

This optimization problem is formulated to minimize the mean square error while guaranteeing the convergence of the method that maximizes system performance [27]. We employ the PSO algorithm to solve this problem and determine the optimal ω and γ. PSO is a powerful and popular metaheuristic optimization algorithm that simulates the intelligent behavior of a swarm to navigate a complex search space and find optimal solutions.

Mapping the problem to PSO [28]:

- Particle. Each particle in the swarm represents a candidate solution.
- Particle position. It is a vector of the parameters we want to optimize. In this case $\text{position\_X} = [\omega_X, \gamma_X]$.
- Search space. We need to define the valid range for ω and γ and these parameters must be within the range of $[0, 2]$ for convergence.
- Fitness function. This is the most critical part. The fitness function evaluates how good a particle's position $[\omega, \gamma]$ is.

The flow chart of the basic PSO is depicted in Fig. 2.

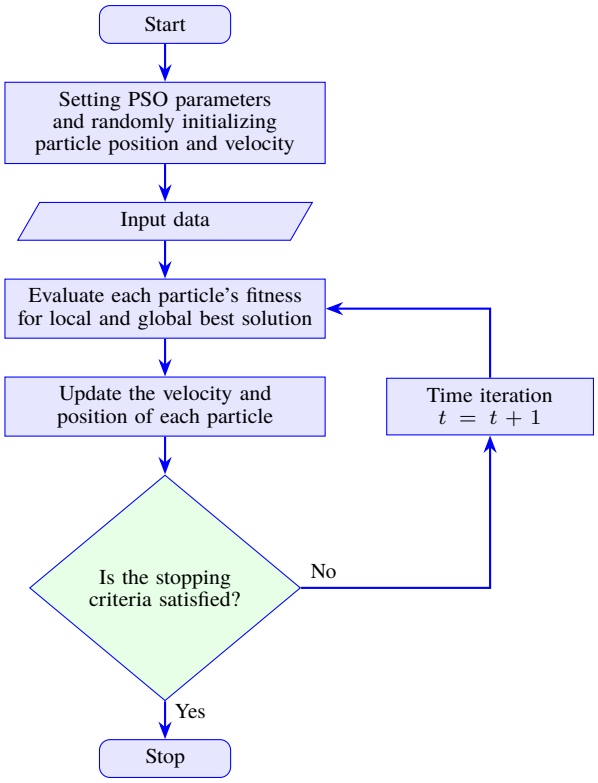

Fig. 2. Particle swarm optimization flow chart.

At each iteration $t+1$, every particle p updates its velocity V and position X. The process is defined by the following velocity and position update equations [29]:

$$V^{(t+1)} = \Omega\, V^{(t)} + c_1\, r_1 \left(p_{best}^{(t)} - X^{(t)}\right) + c_2\, r_2 \left(g_{best}^{(t)} - X^{(t)}\right), \tag{32}$$

$$X^{(t+1)} = X^{(t)} + V^{(t+1)}, \tag{33}$$

where Ω is the inertia weight, c_1 and c_2 are the cognitive acceleration coefficients and r_1, r_2 are random numbers uniformly distributed over the interval $[0,1]^D$; D denotes the dimensionality of the search space (i.e., the problem size).

Unlike OAOR, which optimizes parameters only within the standard AOR framework, the proposed OSAOR combines the symmetric SAOR structure with PSO-based parameter selection.

Since symmetric schemes already improve stability and performance over standard AOR, integrating the PSO-based global optimizer at this level enables further gains in convergence speed and SER performance, making OSAOR fundamentally different from the OAOR precoding algorithm.

4. Computational Complexity

Computational complexity of the SAOR-based precoding algorithm is analyzed in terms of the number of complex multiplications required per iteration. The iterative process is dominated by sparse matrix-vector products and forward/backward substitutions. A full symmetric SAOR iteration consists of one forward and one backward pass. In each pass, the update involves calculating:

$$(\gamma - \omega)\, W_L\, x + (1-\omega)\, W_D\, x + \omega\, W_U\, x\,,$$

which requires approximately

$$\frac{U^2 - U}{2} + U + \frac{U^2 - U}{2} = U^2$$

multiplications, where U is the number of users.

This is followed by a forward substitution to solve the system $(W_D - W_L)\, x_{new}$, which requires an additional $\frac{1}{2}(U^2 - U)$ multiplications.

The sum of operations performed during both passes yields a total complexity of approximately $3\,U^2$ complex multiplications per iteration. Therefore, the SAOR algorithm exhibits a computational complexity of $\mathcal{O}(U^2)$. This is a significant advantage over direct matrix inversion methods such as ZF, which are $\mathcal{O}(U^3)$, making SAOR a highly efficient solution for massive MIMO systems. Although its complexity is slightly higher than $\mathcal{O}(2\,U^2)$ of the SSOR method due to an additional matrix vector product, this cost enables the use of a second parameter γ that can accelerate convergence and improve performance, representing a favorable trade-off between computational effort and system accuracy.

The OSAOR-based precoding algorithm combines SAOR iteration with a PSO stage to optimally tune its relaxation and acceleration parameters. The PSO algorithm operates with P particles over T iterations, with fitness evaluation being the most demanding step. A straightforward evaluation involves operations comparable to a SAOR algorithm with complexity of $\mathcal{O}(U^2)$. However, by adopting sampling and approximation, this can be reduced to $\mathcal{O}(U\log(U))$.

Therefore, the overall cost of the PSO phase is $\mathcal{O}(PTU\log(U))$, which is a one-time cost for a given channel realization and does not contribute to each transmission iteration. After optimization, OSAOR precoding proceeds in a manner that is identical to that charcteristic of SAOR, with per-iteration complexity of $\mathcal{O}(U^2)$. Consequently, the overall complexity of OSAOR remains of order $\mathcal{O}(U^2)$, significantly lower than the complexity of ZF precoding, while providing faster convergence and improved error rate performance.

The computational complexity of linear precoding algorithms is summarized in Tab. 1.

5. Results and Discussion

In this section, we numerically analyze and discuss the performance of the proposed precoding method in terms of SER and ergodic capacity with respect to different SNR values and iteration counts. The results are compared with conventional AOR, SSOR, and SAOR-based multi-user precoders over the Rayleigh fading channel.

For reference, the near optimal ZF precoder is also included as a benchmark. Simulations are carried out for a 128×16 BS user antenna configuration in a massive downlink MIMO system using 64-quadrature amplitude modulation (64-QAM). SER results are averaged over 5×10^4 Monte

Tab. 1. Computational complexity of different precoding schemes.

Precoder	Complexity order	Remarks
ZF	$\mathcal{O}(U^3)$	Requires exact matrix inversion
AOR	$\mathcal{O}(U^2)$	Two parameters (relaxation, acceleration)
SSOR	$\mathcal{O}(U^2)$	Single relaxation parameter
SAOR	$\mathcal{O}(U^2)$	Two parameters (relaxation, acceleration)
OSAOR	$\mathcal{O}(U^2)$	PSO overhead: $\mathcal{O}(PTU \log U)$ (one-time), then $\mathcal{O}(U^2)$ per iteration

Tab. 2. PSO parameters used in the simulation.

Parameter	Value
Number of particles P	20
Number of iterations T	15
Inertia weight (max) $\Omega_{\max}$	0.9
Inertia weight (min) $\Omega_{\min}$	0.4
Cognitive coefficient c_1	2.0
Social coefficient c_2	2.0

Carlo trials, while PSO optimization parameters are listed in Tab. 2.

PSO parameters were selected based on values that are widely adopted in the literature and were validated through preliminary simulations. The size of the swarm $P = 20$ and the iteration limit $T = 15$ provide a good trade-off between reliability of convergence and computational cost. The inertia weight was linearly decreased from $\Omega_{max} = 0.9$ to $\Omega_{min} = 0.4$ to balance exploration and exploitation, while the cognitive and social coefficients were set at $c_1 = c_2 = 2.0$, which are canonical choices that ensure stable convergence. Sensitivity tests confirmed that small variations of these parameters do not significantly affect the convergence behavior or final performance, demonstrating the robustness of the adopted setting.

Figure 3 shows the convergence behavior of the PSO algorithm used to find the optimal parameters for the OSAOR precoder. The fitness function which is defined as $\frac{1}{1+error}$ is designed so that as the error of the precoder decreases towards zero, the fitness value approaches its maximum of 1.

The plot shows that the PSO algorithm converges quickly. There is a significant improvement in fitness between the first and second iterations, indicating that the algorithm rapidly identifies a promising region in the parameter space. From the second iteration onward, the fitness value continues to improve in very fine increments, stabilizing, and effectively converging by the 11-th iteration. This rapid convergence highlights the efficiency of using PSO to tune the parameters of OSAOR.

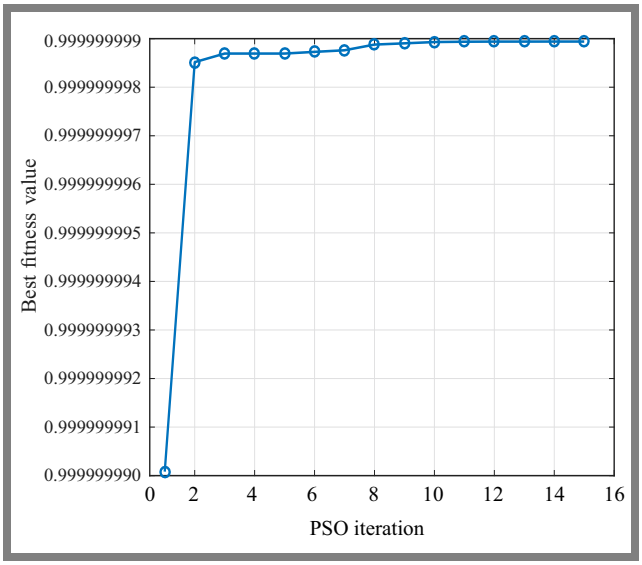

Fig. 3. Convergence of PSO fitness function for optimization of OSAOR parameters.

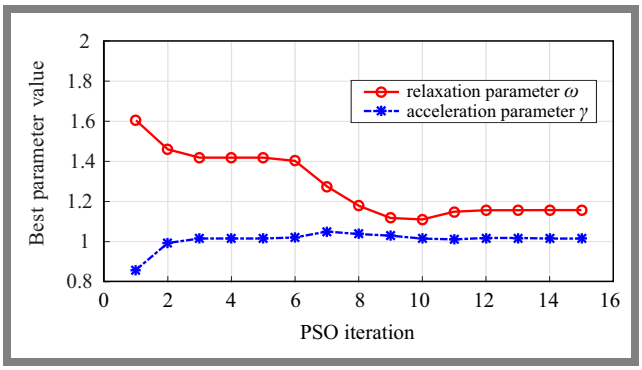

Fig. 4. Evolution of optimal OSAOR parameters ω and γ across PSO iterations.

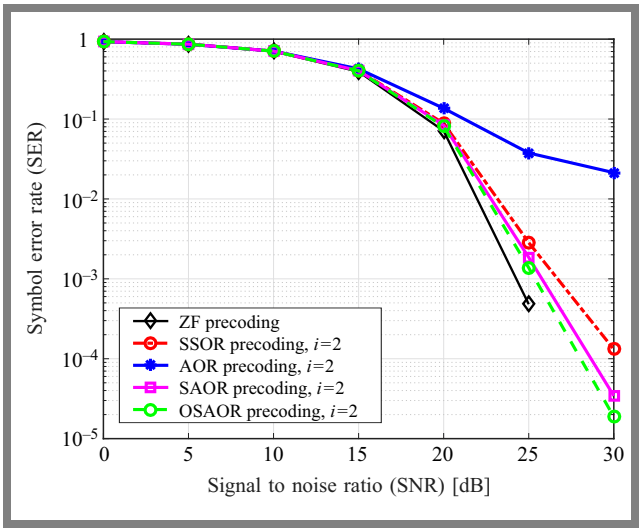

Fig. 5. Comparison of SER vs. SNR performance for a $(N, U) = (128, 16)$ precoding m-MIMO system.

Figure 4 provides the evolution of the two key OSAOR parameters that are being optimized: relaxation parameter ω and acceleration parameter γ. The graph shows that in the initial iterations, particularly for the relaxation parameter ω,

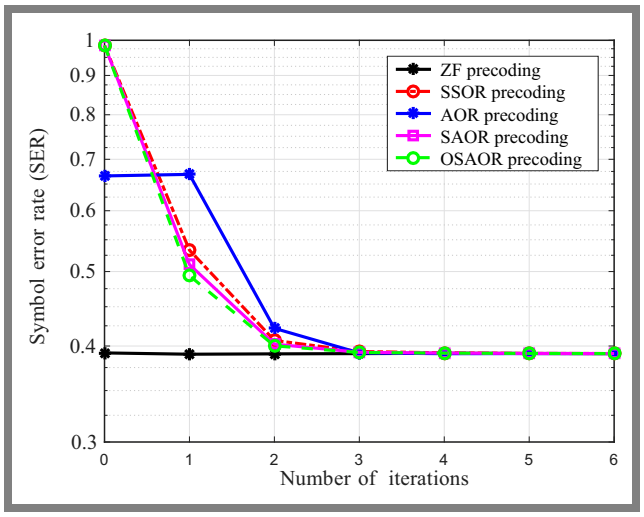

Fig. 6. Comparison of the performance of SER against the number of iterations for a $(N, U) = (128, 16)$ precoding m-MIMO system.

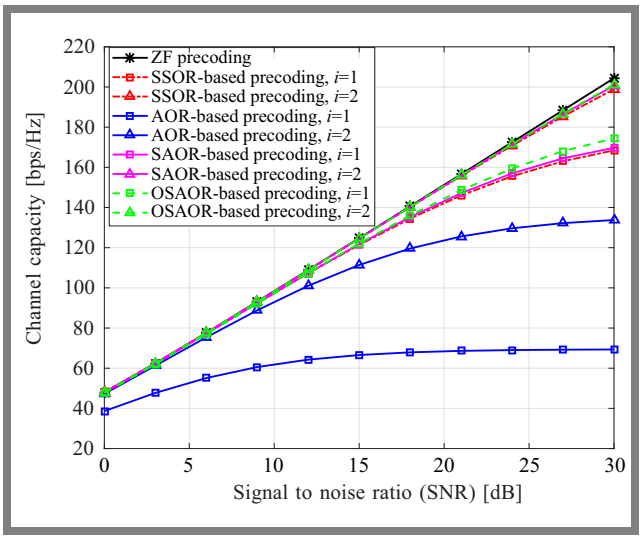

Fig. 7. Comparison of capacity performance of the investigated precoding iterative techniques against the SNR for a $(N, U) = (128, 16)$ m-MIMO system.

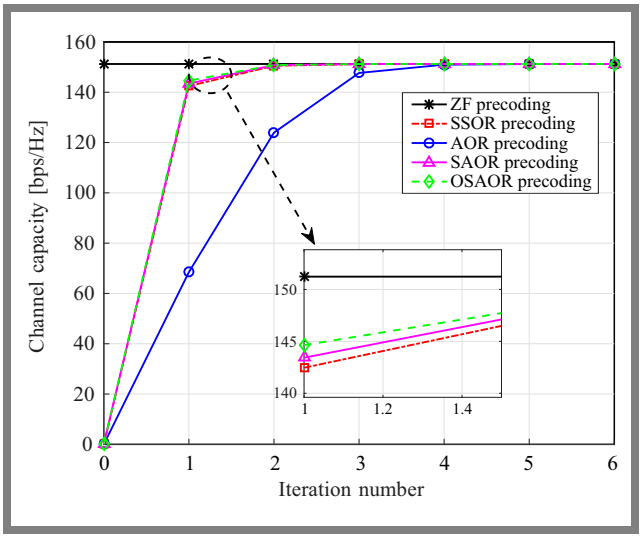

Fig. 8. Comparison of capacity performance of the studied precoding iterative techniques against the number of iterations for a $(N, U) = (128, 16)$ m-MIMO system.

the algorithm makes significant adjustments, starting from approximately 1.6 and decreasing to around 1.1 by iteration 10.

The acceleration parameter γ shows a more modest adjustment, starting near 0.85 and settling around 1.02. After approximately the 10-th iteration, both parameters stabilize, which corresponds directly to the point where the fitness function flattens. This indicates that the PSO algorithm has successfully converged to a stable set of optimal parameters, which are found to be approximately $\omega \simeq 1.15$ and $\gamma \simeq 1.02$ for the given system configuration.

Figure 5 presents the SER performance of the proposed precoding schemes compared to conventional methods for a massive MIMO downlink system with $(N, U) = (128, 16)$ and 64-QAM. As expected, SER decreases as SNR increases for all schemes. The ZF precoder, included as a benchmark, achieves the best performance but at the expense of high computational complexity due to matrix inversion calculations. Among the iterative methods, AOR exhibits the weakest performance, particularly at moderate to high SNR values.

On the contrary, both SSOR and SAOR show significant improvements, with SAOR consistently outperforming SSOR as a result of its acceleration mechanism. In particular, the proposed OSAOR scheme achieves the closest performance to ZF across the entire SNR range, particularly at high SNR, where its SER nearly overlaps with that of ZF. This demonstrates that optimizing SAOR parameters using PSO effectively accelerates convergence and minimizes precoding errors, offering a practical low-complexity alternative to ZF for large-scale MIMO systems.

Figure 6 illustrates the performance of SER versus the number of iterations at SNR = 15 dB. As observed, all iterative precoding methods (SSOR, AOR, SAOR, and OSAOR) start with higher SER but converge rapidly within a few iterations. Notably, OSAOR and SAOR achieve faster convergence, reaching near-optimal performance by the second iteration, whereas SSOR lags in the initial iterations. After approximately three iterations, all methods converge to the same performance level as ZF, demonstrating the efficiency of the proposed OSAOR in reducing complexity while maintaining accuracy.

Channel capacity performance is presented in Fig. 7 as a function of SNR for a $(N, U) = (128, 16)$ precoding massive MIMO system. As expected, the near-optimal ZF precoder achieves the highest capacity across the entire SNR range. Among the iterative schemes, OSAOR- and SAOR-based precoding closely approach the performance of ZF, especially from moderate to high SNR values, while requiring only a small number of iterations.

On the contrary, AOR- and SSOR-based methods exhibit slower capacity growth, with SSOR showing the largest performance gap when compared to ZF. These results confirm that OSAOR provides a favorable trade-off between complexity and spectral efficiency, achieving near-optimal capacity with reduced computational cost.

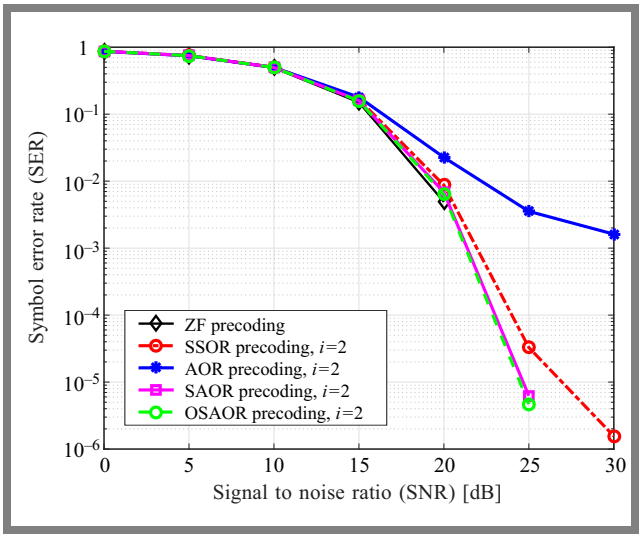

Fig. 9. Comparison of SER performance of the studied precoding iterative techniques against the SNR for a $(N, U) = (256, 32)$ m-MIMO system.

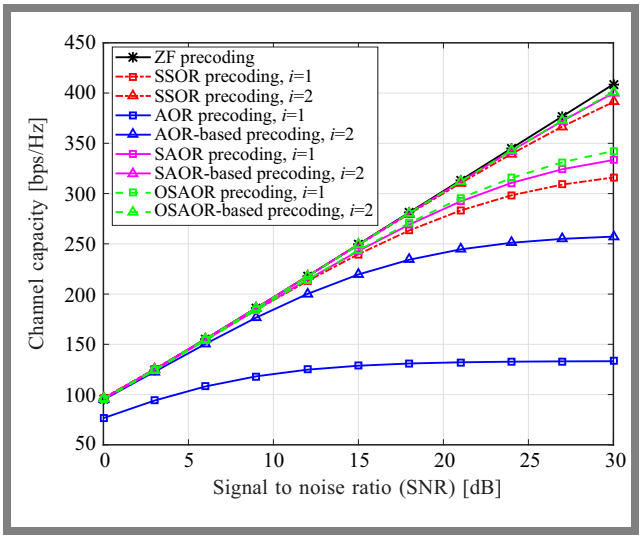

Fig. 10. Comparison of capacity performance of the of the investigated precoding iterative techniques against the SNR for a $(N, U) = (256, 32)$ m-MIMO system.

The convergence performance of several iterative precoding algorithms is illustrated in Fig. 8 by plotting channel capacity against the number of iterations for a massive MIMO system configured with $(N, U) = (128, 16)$ at an SNR of 15 dB. The ZF precoding algorithm serves as a performance benchmark, achieving an optimal channel capacity of approximately 151 bps/Hz. The results clearly demonstrate the superior convergence speed of the symetric-based algorithms (SSOR, SAOR, and OSAOR) over the traditional AOR method. Although the AOR algorithm requires three full iterations to converge to the performance level of ZF, the SSOR, SAOR, and OSAOR schemes achieve near-optimal capacity after just a single iteration and fully converge by the second.

The magnified inset provides a crucial distinction in their first-iteration performance, revealing that the OSAOR algorithm attains the highest capacity, followed closely by SAOR and then SSOR. This signifies that OSAOR offers the most favorable trade-off between computational complexity and performance as it is capable of delivering near-maximum channel capacity with the minimal computational load of a single iteration.

To further evaluate the scalability of the proposed OSAOR algorithm, we extended the simulations to a larger user antenna configuration with $(N, U) = (256, 32)$ using the 32-QAM modulation scheme. Figures 9 and 10 illustrate the resulting SER vs. SNR and achievable capacity vs. SNR, respectively. The results confirm that OSAOR consistently outperforms conventional methods in terms of both error performance and capacity, even under increased system dimensions and other order modulation, thereby demonstrating its robustness and scalability.

6. Conclusions and Future Outlook

By integrating the strengths of the symmetric accelerated over-relaxation (SAOR) method and advantages of the particle swarm optimization (PSO) algorithm, the proposed approach achieves an optimal balance between computational efficiency and SER performance. In addition, the improved version of the standard AOR proposed in this paper achieves a more refined trade-off between performance and complexity compared to basic existing methods.

Furthermore, the simulation results confirm that the proposed OSAOR scheme not only reduces computational load, but also adapts effectively to different system configurations, making it suitable for large-scale deployments. The incorporation of PSO ensures that the relaxation and acceleration parameters are tuned optimally, enabling the algorithm to converge faster and achieve improved error performance.

As this study is limited to simulation-based analysis, future research will extend the scope of the evaluation to cover imperfect CSI scenarios in order to assess the robustness of the proposed method under more realistic channel conditions. Additional performance metrics such as latency, energy efficiency, and computational resource consumption will also be investigated to provide a more comprehensive view of practical applicability.

Furthermore, future work will include hardware-in-the-loop validation and prototype implementations on FPGA/ASIC platforms to evaluate the feasibility of real-time deployment in 5G and beyond wireless systems. Finally, real-time implementation on commercial SDR platforms, followed by field trials, is planned to further confirm the practicality and robustness of the proposed OSAOR scheme under real-world deployment conditions.

Acknowledgments

The work has been funded under the PRFU research project no. A25N01UN300120220001 of the Algerian Ministry of Higher Education and Scientific Research (MESRS).

References

[1] S. Labed and N. Aounallah, "Efficient Iterative Detection Based on Conjugate Gradient and Successive Over-relaxation Methods for Uplink Massive MIMO Systems", *Journal of Telecommunications and Information Technology*, vol. 92, pp. 1–9, 2023 (https://doi.org/10.26636/jtit.2023.169023).

[2] T.A. Sheikh, J. Bora, and M.A. Hussain, "Combined User and Antenna Selection in Massive MIMO Using Precoding Technique", *International Journal of Sensors, Wireless Communications and Control*, vol. 9, pp. 214–223, 2019 (https://doi.org/10.2174/2210327908666181112144939).

[3] S. Buzzi, C. D'Andrea, A. Zappone, and C. D'Elia, "User-centric 5G Cellular Networks: Resource Allocation and Comparison with the Cell-free Massive MIMO Approach", *IEEE Transactions on Wireless Communications*, vol. 19, pp. 1250–1264, 2020 (https://doi.org/10.1109/TWC.2019.2952117).

[4] M. Costa, "Writing on Dirty Paper", *IEEE Transactions on Information Theory*, vol. 29, pp. 439–441, 1983 (https://doi.org/10.1109/TIT.1983.1056659).

[5] M. Mazrouei-Sebdani, W.A. Krzymień, and J. Melzer, "Massive MIMO with Nonlinear Precoding: Large-system Analysis", *IEEE Transactions on Vehicular Technology*, vol. 65, pp. 2815–2820, 2016 (https://doi.org/10.1109/TVT.2015.2425884).

[6] E. Björnson and L. Sanguinetti, "Making Cell-free Massive MIMO Competitive with MMSE Processing and Centralized Implementation", *IEEE Transactions on Wireless Communications*, vol. 19, pp. 77–90, 2020 (https://doi.org/10.1109/TWC.2019.2941478).

[7] A. Björck, *Numeric Methods in Matrix Computations*, Springer, 816 p., 2015 (https://doi.org/10.1007/978-3-319-05089-8).

[8] X. Gao, L. Dai, Y. Ma, and Z. Wang, "Low-complexity Near-optimal Signal Detection for Uplink Large-scale MIMO Systems", *Electronics Letters*, vol. 50, pp. 1326–1328, 2014 (https://doi.org/10.1049/el.2014.0713).

[9] B. Yin, M. Wu, J.R. Cavallaro, and W. Studer, "Conjugate Gradient-based Soft-output Detection and Precoding in Massive MIMO Systems", *IEEE Global Communications Conference (GLOBECOM)*, Austin, USA, 2014 (https://doi.org/10.1109/GLOCOM.2014.7037382).

[10] L. Dai *et al.*, "Low-complexity Soft-output Signal Detection Based on Gauss-Seidel Method for Uplink Multiuser Large-scale MIMO Systems", *IEEE Transactions on Vehicular Technology*, vol. 64, pp. 4839–4845, 2015 (https://doi.org/10.1109/TVT.2014.2370106).

[11] D. Zhu, B. Li, and P. Liang, "On the Matrix Inversion Approximation Based on Neumann Series in Massive MIMO Systems", *IEEE International Conference on Communications (ICC)*, London, UK, 2015 (https://doi.org/10.1109/ICC.2015.7248580).

[12] C. Tang, C. Liu, L. Yuan, and Z. Xing, "High Precision Low Complexity Matrix Inversion Based on Newton Iteration for Data Detection in the Massive MIMO", *IEEE Communications Letters*, vol. 20, pp. 490–493, 2016 (https://doi.org/10.1109/LCOMM.2015.2514281).

[13] C. Zhang *et al.*, "A Low-complexity Massive MIMO Precoding Algorithm based on Chebyshev Iteration", *IEEE Access*, vol. 5, pp. 22545–22551, 2017 (https://doi.org/10.1109/ACCESS.2017.2760881).

[14] M.A. Albreem, M. Juntti, and S. Shahabuddin, "Massive MIMO Detection Techniques: A Survey", *IEEE Communications Surveys & Tutorials*, vol. 21, pp. 3109–3132, 2019 (https://doi.org/10.1109/COMST.2019.2935810).

[15] M.A. Albreem, A.H.A. Habbash, A.M. Abu-Hudrouss, and S.S. Ikki, "Overview of Precoding Techniques for Massive MIMO", *IEEE Access*, vol. 9, pp. 60764–60801, 2021 (https://doi.org/10.1109/ACCESS.2021.3073325).

[16] A. Hadjidimos, "Accelerated Overrelaxation Method", *Mathematics of Computation*, vol. 32, pp. 149–157, 1978.

[17] Y. Hu, J. Wu, and Y. Wang, "SAOR-based Precoding with Enhanced BER Performance for Massive MIMO Systems", *International Conference on Artificial Intelligence in Information and Communication (ICAIIC)*, Okinawa, Japan, 2019 (https://doi.org/10.1109/ICAIIC.2019.8668984).

[18] J. Wu, Y. Hu, and Y. Wang, "An Improved AOR-based Precoding for Massive MIMO Systems", *Proc. of 4th International Conference on Communication and Information Processing*, pp. 251–255, 2018 (https://doi.org/10.1145/3290420.3290427).

[19] M.N. Irshad, I.A. Khoso, M.M. Aslam, and M. Silapunt, "Optimized Accelerated Over-relaxation Method for Robust Signal Detection: A Metaheuristic Approach", *Algorithms*, vol. 17, art. no. 463, 2024 (https://doi.org/10.3390/a17100463).

[20] M.N. Irshad, M.M. Aslam, and R. Silapunt, "Low Complexity Optimized AOR Method for Massive MIMO Signal Detection", *IEEE Access*, vol. 13, pp. 51054–51068, 2025 (https://doi.org/10.1109/ACCESS.2025.3550272).

[21] T.L. Marzetta, "Noncooperative Cellular Wireless with Unlimited Numbers of Base Station Antennas", *IEEE Transactions on Wireless Communications*, vol. 9, pp. 3590–3600, 2010 (https://doi.org/10.1109/TWC.2010.092810.091092).

[22] L. Yang *et al.*, "Low-complexity and Fast-convergence Linear Precoding Based on Modified SOR for Massive MIMO Systems", *Digital Signal Processing*, vol. 107, art. no. 102864, 2020 (https://doi.org/10.1016/j.dsp.2020.102864).

[23] N. Aounallah, "Initialization of an Iterative Low-complexity Method for Signal Precoding in MM-Wave Massive MIMO Systems", *Traitement du Signal*, vol. 40, pp. 361–366, 2023 (http://doi.org/10.18280/ts.400136).

[24] A.E. Zorkun, M.A. Salas-Natera, and R.M. Rodriguez-Osorio, "Improved Iterative Inverse Matrix Approximation Algorithm for Zero Forcing Precoding in Large Antenna Arrays", *IEEE Access*, vol. 10, pp. 100964–100975, 2022 (https://doi.org/10.1109/ACCESS.2022.3208155).

[25] E. Bobrov, D. Kropotov, S. Troshin, and D. Zaev, "Study on Precoding Optimization Algorithms in Massive MIMO System with Multi-antenna Users", *Optimization Methods and Software*, vol. 39, pp. 282–297, 2024 (https://doi.org/10.1080/10556788.2022.2091564).

[26] Q. Xue, "The Analysis of the Convergence of the AOR Method and the Comparison with the SOR Method", *Numerical Mathematics A Journal of Chinese Universities*, pp. 39–49, 2006.

[27] C.L. Meng and C.C. Shen, "PSO-based Searching Precoding for MU-MIMO System", *Wireless Personal Communications*, vol. 135, pp. 1845–1860, 2024 (https://doi.org/10.1007/s11277-024-11170-8).

[28] W.B. Abbas, *et al.*, "Heuristic Antenna Selection and Precoding for a Massive MIMO System", *IEEE Open Journal of the Communications Society*, vol. 5, pp. 83–96, 2024 (https://doi:10.1109/OJCOMS.2023.3339402).

[29] A.G. Gad, "Particle Swarm Optimization Algorithm and its Applications: A Systematic Review", *Archives of Computational Methods in Engineering*, vol. 29, pp. 2531–2561, 2022 (https://doi.org/10.1007/s11831-021-09694-4).

Naceur Aounallah, Prof.
Department of Electronic and Telecommunications
https://orcid.org/0000-0001-9137-7900
E-mail: aounallah.naceur@univ-ouargla.dz
Kasdi Merbah Ouargla University, Ouargla, Algeria
https://www.univ-ouargla.dz

Smail Labed, M.Sc.
Electrical Engineering Laboratory (LAGE)
https://orcid.org/0000-0003-1317-8572
E-mail: labed.smail@univ-ouargla.dz
Kasdi Merbah Ouargla University, Ouargla, Algeria
https://www.univ-ouargla.dz